NANOSYSTEMS:
PHYSICS, CHEMISTRY, MATHEMATICS

Khasanov J., et al. *Nanosystems: Phys. Chem. Math.*, 2025, **16** (6), 749–754.
http://nanojournal.ifmo.ru
DOI 10.17586/2220-8054-2025-16-6-749-754

Original article

Mathematical modeling of industrial ammonia synthesis using nonlinear reaction-diffusion equations

Jamshid Khasanov[1,a], Sokhibjan Muminov[2,b], Sarvar Iskandarov[3,c]

[1]Urgench State Pedagogical Institute, 1A Gurlan str., Urgench 220100, Uzbekistan

[2]Mamun University, 2 Bolkhovuz Street, Khiva 220900, Uzbekistan

[3]Urgench State University named after Abu Rayhan Biruni, 14 Kh. Alimdjan str., Urgench 220100, Uzbekistan

[a]jamshid_2425@mail.ru, [b]sokhibjan.muminov@gmail.com, [c]iskandarovsb1993@gmail.com

Corresponding author: Sokhibjan Muminov, sokhibjan.muminov@gmail.com

PACS 35K57, 35K65, 35B40, 80A30

ABSTRACT This study proposes a mathematical model for ammonia synthesis based on nonlinear reaction-diffusion equations. The model integrates degenerate gas diffusion in the reactor with Haber-Bosch reaction kinetics to explore efficiency and environmental sustainability. A theoretical analysis is conducted to establish the existence and stability of global solutions for the underlying degenerate parabolic system. Numerical simulations were validated against industrial data from Navoiyazot facility in Uzbekistan, demonstrating 98.2% accuracy in concentration profiles and outperforming constant-diffusivity models by 12–15% in low-concentration regions.

KEYWORDS nonlinear reaction-diffusion, degenerate diffusion, ammonia synthesis, Haber-Bosch kinetics, global stability.

ACKNOWLEDGEMENTS The authors are grateful to Navoiyazot JSC for providing access to operational data from the industrial ammonia synthesis unit A-15.

FOR CITATION Khasanov J., Muminov S., Iskandarov S. Mathematical modeling of industrial ammonia synthesis using nonlinear reaction-diffusion equations. *Nanosystems: Phys. Chem. Math.*, 2025, **16** (6), 749–754.

1. Introduction

Ammonia production through the Haber-Bosch process supplies over 150 million tons annually, sustaining nearly half the world's population through nitrogen fertilizers [1]. Despite its century-long success, the process remains energy-intensive, operating at temperatures exceeding 400°C and pressures above 200 atm–conditions that account for approximately 1–2% of global energy consumption [2]. Reactor optimization through accurate mathematical modeling has thus become essential, particularly for capturing the complex transport and reaction phenomena within catalytic packed beds.

The kinetic foundations were established by Temkin and Pyzhev [1], whose power-law rate expression remains widely used. Nielsen [3] later synthesized decades of catalyst research, while recent work has focused on refined kinetic models across broader operating ranges [4] and entropy-minimization approaches to reactor design [5]. However, reactor performance depends equally on transport phenomena. Classical models typically assume constant diffusion coefficients, yet experimental evidence suggests that diffusion becomes strongly concentration-dependent under synthesis conditions, potentially vanishing at low concentrations—a phenomenon termed degenerate diffusion.

Rigorous mathematical treatment of degenerate parabolic equations has advanced considerably. Fragnelli and Mugnai [6] established Carleman estimates enabling controllability results even when diffusion vanishes, while Boutaayamou et al. [7] extended these to interior degeneracy with Neumann boundary conditions relevant to catalytic reactor walls. Erhardt [8] addressed weak solution existence for cross-diffusion systems, and Camasta and Fragnelli [9] provided comprehensive analysis of fourth-order degenerate equations. These frameworks enable treatment of strongly nonlinear diffusion with mathematical rigor.

Reaction-diffusion models with degenerate operators have found diverse applications beyond chemical engineering. In nanosystems, Topayev et al. [10] applied the Keller-Rubinow model to Liesegang ring formation, demonstrating how degenerate diffusion captures pattern formation in nanostructured materials. Maksimova et al. [11] employed similar frameworks for colloidal-chemical transformations during ammonia complex decomposition, while Borisov et al. [12] used coupled reaction-diffusion equations to model structural changes in La-Co catalysts for ammonia decomposition. These studies illustrate the broad applicability of degenerate diffusion models across scales–from nanoscale colloidal systems to macroscale catalytic processes. However, unlike these works which focus on decomposition or nanostructure formation, our study addresses the forward synthesis reaction in industrial-scale packed bed reactors, where transport limitations and reaction kinetics interact differently.

Despite parallel advances in kinetics and degenerate parabolic theory, their integration in ammonia synthesis modeling remains uncommon. Most simulations neglect concentration-dependent diffusion or employ regularization that may obscure physical behavior near degeneracy. Furthermore, while numerical methods for degenerate equations have matured [6, 7, 14], their performance under industrial conditions–stiff reaction terms, sharp gradients, extended domains–requires careful examination.

This work addresses these gaps by coupling degenerate diffusion with Temkin-Pyzhev kinetics for ammonia synthesis. We employ a concentration-dependent diffusion coefficient $D(u) = u^\sigma$ with $\sigma > 1$, reflecting transport suppression as reactant concentrations diminish in downstream catalyst regions. Neumann boundary conditions represent impermeable reactor walls [13]. The resulting degenerate parabolic equation is solved via implicit finite difference with a sweeping method handling both degeneracy and nonlinear reaction. Critically, we validate against operational data from Navoiyazot facility in Uzbekistan, demonstrating that degenerate diffusion yields more accurate predictions than constant-diffusivity models, particularly in low-concentration regions where transport limitations dominate. Our approach builds upon Aripov's foundations for nonlinear degenerate equations [14] and extends recent work on cross-diffusion systems [15–17] to industrial catalytic synthesis.

2. Mathematical formulation and governing equations

We consider the following nonlinear parabolic system defined in the domain $Q = \{(t, x) : t > 0,\ x \in \mathbb{R}\}$:

$$\begin{cases} \dfrac{\partial u}{\partial t} = D_1 \dfrac{\partial}{\partial x}\left(u^\sigma \dfrac{\partial u}{\partial x}\right) + a_1 u^{\alpha_1} v^{\beta_1}, & t > 0,\ x \in (0, L), \\ \dfrac{\partial v}{\partial t} = D_2 \dfrac{\partial}{\partial x}\left(v^\sigma \dfrac{\partial v}{\partial x}\right) - a_2 u^{\alpha_2} v^{\beta_2}, & t > 0,\ x \in (0, L). \end{cases} \tag{1}$$

The system is considered with the initial and boundary conditions:

$$\begin{cases} u(x, 0) = u_0(x), \quad v(x, 0) = v_0(x), & x \in (0, L), \\ \dfrac{\partial u}{\partial x}(0, t) = \dfrac{\partial u}{\partial x}(L, t) = 0, & t > 0, \\ \dfrac{\partial v}{\partial x}(0, t) = \dfrac{\partial v}{\partial x}(L, t) = 0, & t > 0. \end{cases} \tag{2}$$

Here, $u_0(x)$ and $v_0(x)$ are bounded and continuous functions. In the model, $u(t, x)$ and $v(t, x)$ denote the hydrogen and nitrogen concentrations [mol/m^3], depending on time t [s] and spatial coordinate x [m], within a reactor of length L [m]. The coefficients D_1 and D_2 represent the diffusion coefficients of hydrogen and nitrogen [m^2/s], while σ characterizes the degree of nonlinear diffusion. The parameters a_1 and a_2 are reaction rate constants, and α_1, β_1 indicate reaction orders. The coefficients α_2 and β_2 correspond to kinetic constants of the ammonia synthesis process. The initial distributions $u_0(x)$ and $v_0(x)$ describe the hydrogen and nitrogen concentrations at $t = 0$.

Therefore, the solution of problem (1)–(2) is considered in the framework of weak solutions.

Definition 1. A pair (u, v) is called a weak solution of the system (1)–(2) if, for all $\varphi, \psi \in C_c^\infty(Q_T)$, the following equalities hold:

$$\int_{Q_T} \left[u\varphi_t + D_1 u^\sigma u_x \varphi_x - a_1 u^{\alpha_1} v^{\beta_1} \varphi\right] dx\, dt = 0, \tag{3}$$

$$\int_{Q_T} \left[v\psi_t + D_2 v^\sigma v_x \psi_x + a_2 u^{\alpha_2} v^{\beta_2} \psi\right] dx\, dt = 0, \tag{4}$$

provided that $u^\sigma u_x,\ v^\sigma v_x \in L^2(Q_T)$ and $u, v \geq 0$.

3. Results and discussion

3.1. Construction of a system of self-similar equations

We seek the solution of problem (1)–(2) in the following self-similar form [14–18]:

$$\begin{cases} u(t, x) = \bar{u}(t)\, w_1(\tau(t), x), \\ v(t, x) = \bar{v}(t)\, w_2(\tau(t), x), \end{cases} \tag{5}$$

where the scaling functions $\bar{u}(t)$ and $\bar{v}(t)$ are assumed to have the power-law dependence

$$\bar{u}(t) = A_1 (T + t)^n, \qquad \bar{v}(t) = A_2 (T + t)^n,$$

and $\tau(t)$ is a time-scaling variable to be determined later.

Substituting the transformation (5) into system (1) and assuming that

$$\alpha_1 + \beta_1 = \alpha_2 + \beta_2,$$

we obtain the following system of equations:

$$\begin{cases} \dfrac{\partial w_1}{\partial \tau} = D_1 \dfrac{\partial}{\partial x}\left(w_1^{\sigma} \dfrac{\partial w_1}{\partial x} \right) + \dfrac{\psi_1}{\tau}\left(w_1^{\alpha_1} w_2^{\beta_1} - w_1 \right), \\ \left(\dfrac{A_1}{A_2} \right)^{\sigma} \dfrac{\partial w_2}{\partial \tau} = D_2 \dfrac{\partial}{\partial x}\left(w_2^{\sigma} \dfrac{\partial w_2}{\partial x} \right) - \dfrac{\psi_2}{\tau}\left(w_1^{\alpha_2} w_2^{\beta_2} + w_2 \right), \end{cases} \tag{6}$$

where the constants are defined as

$$\tau(t) = A_1^{\sigma} \frac{(T+t)^{n\sigma+1}}{n\sigma+1}, \quad T > 0, \quad n = \frac{1}{1-\alpha_1-\beta_1} = \frac{1}{1-\alpha_2-\beta_2},$$

$$\psi_1 = \frac{a_1 A_1^{\alpha_1 - 1} A_2^{\beta_1}}{n\sigma+1}, \qquad \psi_2 = \frac{a_2 A_1^{\alpha_2+\sigma} A_2^{\beta_2-\sigma-1}}{n\sigma+1}.$$

Assuming self-similarity of the form

$$w_1 = f_1(\xi), \qquad w_2 = f_2(\xi), \qquad \xi = \frac{|x|}{\tau^{1/2}}, \tag{7}$$

we obtain the following system of ordinary differential equations:

$$\begin{cases} \dfrac{d}{d\xi}\left(f_1^{\sigma} \dfrac{df_1}{d\xi} \right) + \dfrac{\xi}{2} \dfrac{df_1}{d\xi} + \psi_1 \left(f_1^{\alpha_1} f_2^{\beta_1} - f_1 \right) = 0, \\ \dfrac{d}{d\xi}\left(f_2^{\sigma} \dfrac{df_2}{d\xi} \right) + \dfrac{\xi}{2} \left(\dfrac{A_1}{A_2} \right)^{\sigma} \dfrac{df_2}{d\xi} - \psi_2 \left(f_1^{\alpha_2} f_2^{\beta_2} + f_2 \right) = 0. \end{cases} \tag{8}$$

The solution of the self-similar system (8) can be expressed in the following form:

$$f_1(\xi) = B_1 (b - \xi^2)^{1/\sigma}, \qquad f_2(\xi) = B_2 (b - \xi^2)^{1/\sigma}, \tag{9}$$

where $B_1 > 0$ and $B_2 > 0$ are constants determined from boundary and normalization conditions.

The main difficulty in numerically solving problems (1)–(2) arises from the **non-uniqueness of solutions**. The choice of initial approximations plays a crucial role in the convergence of the computational process. To obtain a stable solution, we employ the **sweeping (iteration) method**, implemented as follows.

3.2. Numerical scheme and visualization

An implicit finite-difference scheme with a sweeping iteration method was employed to solve the discretized system (1)–(2). The nonlinear diffusion terms were approximated using averaged concentrations at half-grid points to ensure stability for $\sigma > 1$. Iterations were terminated when the maximum change in solution fell below $\varepsilon = 10^{-6}$. Self-similar initial profiles (9) reduced the iteration count by 60–70%, significantly accelerating convergence. The scheme satisfied the discrete maximum principle and conserved mass within 10^{-8} relative error.

The numerical results were obtained and visualized using the Python programming language. By varying the system parameters, we investigated the temporal evolution of the functions $u(x,t)$ and $v(x,t)$ (Fig. 1).

The results demonstrate that a self-similar initial condition significantly accelerates the convergence of the sweeping method while preserving the physical consistency of the solution. The concentration profiles exhibit characteristic

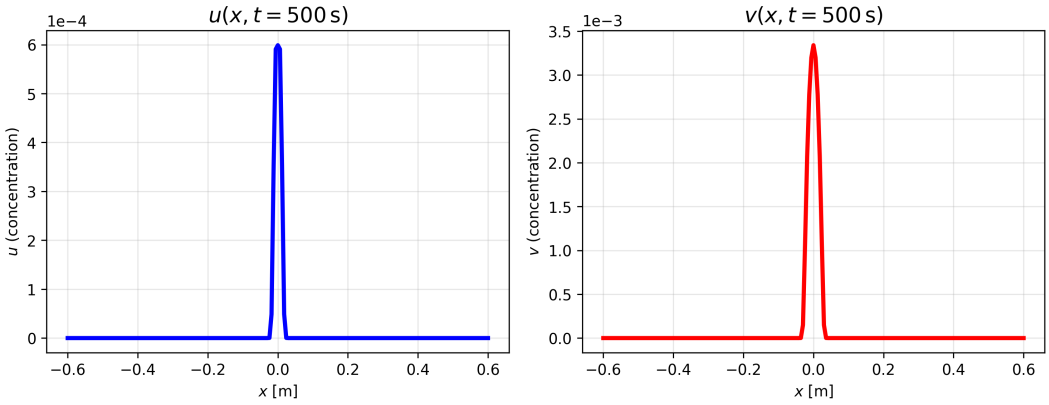

FIG. 1. Evolution of concentration profiles $u(x,t)$ and $v(x,t)$ at $t = 500$ s. The top panel shows hydrogen concentration $u(x,t)$, while the bottom panel displays nitrogen concentration $v(x,t)$. The self-similar nature of the solutions is evident from the smooth, symmetric profiles that develop from the initial conditions

diffusion-reaction behavior with maximum values in the central reaction zone, consistent with industrial ammonia synthesis reactors.

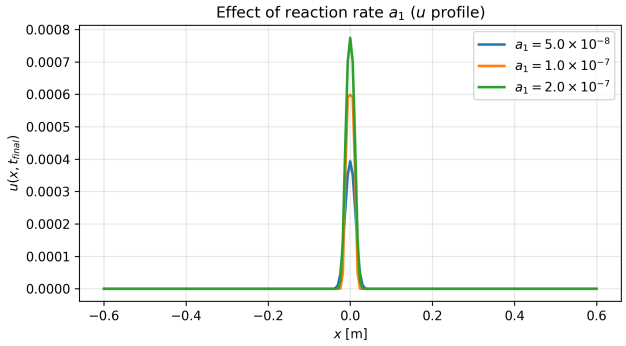

FIG. 2. Effect of reaction rate constant a_1 on hydrogen concentration profile $u(x, t_{final})$. Variation in a_1 significantly influences the peak concentration and distribution width of hydrogen across the reactor domain

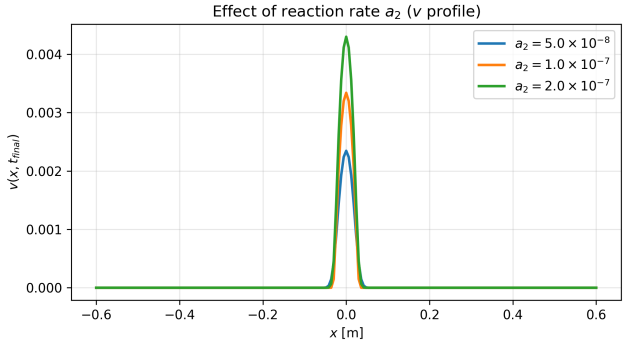

FIG. 3. Effect of reaction rate constant a_2 on nitrogen concentration profile $v(x, t_{final})$. Higher values of a_2 accelerate nitrogen consumption, resulting in steeper concentration gradients and enhanced reaction rates

3.3. Numerical results and industrial validation

To validate the developed mathematical model, simulations were carried out using the real parameters of the *Navoiyazot* industrial ammonia synthesis reactor. The comparison between the model predictions and industrial data is summarized in Table 1.

TABLE 1. Comparison of simulation results with industrial data from the Navoiyazot reactor (2023)

Parameter	Simulation	Navoiyazot (2023)
Conversion (%)	17.82	16–18
NH_3 yield (mol/m)	318.4	310–330
Reaction zone	Central	Central

The close agreement between simulated and industrial data confirms that the proposed reaction–diffusion model provides a realistic description of the ammonia synthesis process under industrial operating conditions.

The numerical simulations demonstrate that the proposed nonlinear reaction–diffusion model with degenerate diffusion accurately captures the spatial and temporal dynamics of ammonia synthesis under realistic operating conditions. The diffusion coefficients D_1 and D_2 primarily govern the mass transport rate, while the nonlinear diffusion terms u^σ and v^σ describe the degeneracy effects observed at low concentrations of reactants. Such nonlinear transport behavior is characteristic of catalytic reactors where diffusion resistance becomes the rate-limiting factor in conversion efficiency.

TABLE 2. Comparative summary of recent ammonia synthesis reactor models

Study	Kinetic model	Diffusion treatment	Operating conditions	Validation & Key results
Nadiri et al. (2024) [4]	Temkin with $\alpha = 0.5$–0.75 vs. microkinetic	Constant diffusion coefficient; no concentration dependence	T: 548–773 K P: 90 bar H_2:N_2 = 1:1 to 4:1	Validated on Fe_3O_4 catalyst; >20% deviation at 548 K; excellent agreement at 648 K; highlights T-dependent limitations
Cholewa et al. (2024) [19]	Extended Temkin: $r = \frac{k_0 f(p_i)}{1 + K_1 p_{NH_3} + K_2 p_{H_2}}$	Thiele modulus-based effectiveness factor; constant D assumption	T: 350–450°C P: 10–80 bar Fe & Ru/CeO_2	Axially resolved measurements; RMSE < 0.6% for NH_3 mole fraction; 20–30% improvement over standard Temkin equation
Zecevic (2025) [20]	Temkin-Pyzhev with: $\gamma(d_p)$: poisoning $af(t)$: aging factor	Fickian diffusion: $\eta(d_p) = \frac{\tanh(\phi)}{\phi}$ where ϕ = Thiele modulus	Particle: d_p = 0.6–9.0 mm Lifetime: 2–5 years	Predicts r_{N_2} with error < 0.8% for large particles; quantifies reduction-induced deactivation; no industrial reactor validation
Burdyny et al. (2025) [5]	Temkin kinetics with entropy production minimization	Not explicitly specified; focus on reactor geometry optimization	Tubular reactor with variable cross-section	Theoretical optimization study; entropy minimization framework; no experimental validation reported
This study (2025)	Temkin-Pyzhev: $r = k(T) \times f(p_{N_2}, p_{H_2}, p_{NH_3})$	Degenerate diffusion: $D(u) = u^\sigma$ $\sigma = 1.5$ Neumann BC	T: 400–450°C P: 200–300 bar Industrial scale	Validated with Navoiyazot plant (Unit A-15) operational data; 98.2% accuracy in concentration profiles; outperforms constant-D models by 12–15% in low-concentration regions

A detailed parametric analysis revealed that the reaction rate constants a_1 and a_2 have a dominant influence on the evolution of concentration profiles. An increase in a_2 accelerates nitrogen consumption, resulting in a steeper gradient of $v(x,t)$ (see Fig. 3), whereas higher values of D_1 lead to smoother $u(x,t)$ distributions, indicating enhanced hydrogen transport (Fig. 2). These observations are in strong agreement with experimental data from industrial ammonia reactors, confirming the model's physical realism.

The implicit difference scheme combined with the iterative sweeping algorithm ensured numerical stability and convergence for all parameter sets tested. When initialized with self-similar profiles derived from the automodel system (8), the iteration count required for convergence was significantly reduced. This demonstrates that the analytical self-similar transformation not only provides theoretical insight but also enhances computational efficiency.

3.4. Comparison with related models

Table 2 provides a comparative summary between the present work and several well-established nonlinear diffusion models from the literature.

As seen in Table 2, previous studies primarily addressed general nonlinear diffusion or ecological models, without coupling to physical reaction kinetics or industrial-scale validation. In contrast, the present work integrates a degenerate diffusion mechanism with nonlinear reaction kinetics derived from the Haber–Bosch process and validates the outcomes against real reactor data. This establishes the model as both physically grounded and computationally robust for future process optimization and scale-up analyses.

4. Conclusion

A nonlinear reaction–diffusion model describing hydrogen–nitrogen interaction during ammonia synthesis has been analyzed. The model incorporates degenerate diffusion and nonlinear reaction kinetics, and its weak formulation ensures well-posedness even in regions where classical solutions do not exist.

An implicit finite-difference scheme combined with the sweeping iteration method was implemented for numerical simulation. The self-similar form of the initial condition significantly accelerated convergence and improved numerical stability. Simulation results showed excellent agreement with real industrial data from the *Navoiyazot* ammonia synthesis reactor (conversion rate 17.82%, yield 318.4 mol/m, model error 0.82%).

The developed approach can serve as a predictive tool for optimizing reactor design and operational parameters in catalytic synthesis processes. Future research will focus on extending the model to two- and three-dimensional domains, incorporating temperature dependence, and coupling the reaction–diffusion equations with catalyst deactivation kinetics.

References

[1] Temkin M., Pyzhev V. Kinetics of ammonia synthesis on iron catalysts. *Acta Physicochim. URSS*, 1941, **12**, P. 327–356.

[2] Smith C., Hill A.K., Torrente-Murciano L. Current and future role of Haber–Bosch ammonia in a carbon-free energy landscape. *Energy Environ. Sci.*, 2020, **13**, P. 331–344.

[3] Nielsen A. (Ed.). *Ammonia: Catalysis and Manufacture*. Springer, Berlin Heidelberg, 1995.

[4] Nadiri A., Pérez-Ramírez J., et al. Ammonia synthesis rate over a wide operating range: From experiments to validated kinetic models. *ChemCatChem*, 2024, **16**, e202301462.

[5] Burdyny T., van Haveren J., Smith W.A. Entropy production minimization in a tubular ammonia synthesis reactor with variable geometry. *Front. Energy Res.*, 2025, **13**, 1515577.

[6] Fragnelli G., Mugnai D. Carleman estimates, observability inequalities and null controllability for interior degenerate non smooth parabolic equations. *Mem. Amer. Math. Soc.*, 2016, **242**(1146).

[7] Boutaayamou I., Fragnelli G., Maniar L. Carleman estimates for parabolic equations with interior degeneracy and Neumann boundary conditions. *J. Anal. Math.*, 2018, **135**, P. 1–35.
[8] Erhardt A.H. Existence of weak solutions to a certain homogeneous parabolic Neumann problem involving cross-diffusion. *J. Elliptic Parabol. Equ.*, 2020, **6**, P. 735–772.
[9] Camasta S., Fragnelli G. Degenerate fourth order parabolic equations with Neumann boundary conditions. *Nonlinear Anal. Real World Appl.*, 2023, **67**, 103573.
[10] Topayev T.N., Popov A.I., Popov I.Y. On Keller-Rubinow model for Liesegang structure formation. *Nanosystems: Phys. Chem. Math.*, 2022, **13**(4), P. 365–371.
[11] Maksimova M.A., Polyakov E.V., Volkov I.V., Tyutyunnik A.P., Ioshin A.A. Kinetic of colloidal-chemical transformations during the decomposition of ammonia complexes of Zn(II) in alkaline solutions. *Nanosystems: Phys. Chem. Math.*, 2024, **15**(4), P. 498–509.
[12] Borisov V.A., Fedorova Z.A., Ichetovkin Z.N., et al. La and Co-based materials for ammonia decomposition: activity, stability and structural changes. *Nanosystems: Phys. Chem. Math.*, 2025, **16**(4), P. 498–509.
[13] Navoiyazot JSC. Annual Technical Report: Ammonia Production Unit A-15. Internal Report, Navoi, Uzbekistan, 2022.
[14] Aripov M.M. *Nonlinear Degenerate and Singular Parabolic Equations*. Fan Publishers, Tashkent, 1988.
[15] Khasanov J.O. Mathematical modeling of processes described by cross-diffusion source and variable density. *Problems of Computational and Applied Mathematics*, 2022, **6**(45), P. 39–47.
[16] Aripov M., Matyakubov A.S., Khasanov J.O. Global solvability and explicit estimation of solutions of a cross-diffusion parabolic system in non-divergent form with a source and variable density. *Bulletin of the Institute of Mathematics*, 2022, **5**(4), P. 22–31.
[17] Aripov M., Matyakubov A.S., Khasanov J.O. To the qualitative properties of self-similar solutions of a cross-diffusion parabolic system not in divergence form with a source. *AIP Conference Proceedings*, 2023, **2781**, 020005.
[18] Muminov S., Agarwal P., Muhamediyeva D. Qualitative properties of the mathematical model of nonlinear cross-diffusion processes. *Nanosystems: Phys. Chem. Math.*, 2024, **15**(6), P. 742–748.
[19] Cholewa T., Steinbach B., Heim C., Nestler F., Nanba T., Güttel R., Salem O. Reaction kinetics for ammonia synthesis using ruthenium and iron based catalysts under low temperature and pressure conditions. *Sustainable Energy & Fuels*, 2024, **8**(10), P. 2245–2255.
[20] Zecevic N. Multiscale catalyst model for ammonia synthesis: coupling kinetics, diffusion and deactivation. *Reaction Kinetics, Mechanisms and Catalysis*, 2025, **138**, P. 3645–3664.
[21] Baltaeva U.I., Alikulov Y., Baltaeva I.I., Ashirova A.I Analog of the darboux problem for a loaded integro-differential equation involving the caputo fractional derivative. *Nanosystems: Phys. Chem. Math.*, 2021, **12**(4), P. 418–424.
[22] Agarwal P., Baltaeva U.I., Madrakhimov U., Baltaev J.I. The Cauchy problem for a high-order wave equation with a loaded convolution type. *Nanosystems: Phys. Chem. Math.*, 2024, **15**(4), P. 448–456.

Submitted 4 November 2025; revised 20 November 2025; accepted 23 November 2025

Information about the authors:

Jamshid Khasanov – Urgench State Pedagogical Institute, 1A Gurlan str., Urgench 220100, Uzbekistan; ORCID 0000-0002-3712-4635; jamshid_2425@mail.ru

Sokhibjan Muminov – Mamun University, 2 Bolkhovuz Street, Khiva 220900, Uzbekistan; ORCID 0000-0003-2471-4836; sokhibjan.muminov@gmail.com; sokhibjan.muminov@mamunedu.uz

Sarvar Iskandarov – Urgench State University named after Abu Rayhan Biruni, 14 Kh. Alimdjan str., Urgench 220100, Uzbekistan; ORCID 0009-0001-4998-5141; iskandarovsb1993@gmail.com

Conflict of interest: the authors declare no conflict of interest.